Universität Hamburg
DER FORSCHUNG | DER LEHRE | DER BILDUNG

ALFRED-WEGENER-INSTITUT
HELMHOLTZ-ZENTRUM FÜR POLAR- UND MEERESFORSCHUNG

Variability of soil properties in arctic Yedoma landscapes: Relevance for estimation of thermal parameters in models

Bachelor's Thesis

Institut für Bodenkunde
Fachbereich Geowissenschaften
Fakultät für Mathematik, Informatik und Naturwissenschaften (MIN)
Universität Hamburg

submitted by
Oliver Kaufmann
matriculation number: 6436637

Hamburg, November 2018

1st adviser: Prof. Dr. Lars Kutzbach
Universität Hamburg, Institut für Bodenkunde

2nd adviser: PD. Dr. Julia Boike
Alfred-Wegener-Institut für Polar- und Meeresforschung
Forschungsstelle Potsdam

original title

Variability of soil properties in arctic Yedoma landscapes: Relevance for estimation of thermal parameters in models

Writing period

01. 06. 2016 – 02. 11. 2018

Examiner

Prof. Dr. Lars Kurzbach

Advisers

PD. Dr. Julia Boike

Contents

List of Figures

List of Tables

Abstract

Climate models use input parameters from early aggregated measurement data to simulate arctic scenarios. Using coarsly resolved input causes a statisticial uncertainty which gets passed through the rest of the computation process by error propagation.

To identify this extent of this error with regard of thermal properties, soil samples were gathered from three locations on Kurungnakh island in the Lena River Delta, Siberia/Russia. Comparable soil layers were investigated concerning the variability of the share of their soil constituents (air, ice, organic matter, solid matter, water) as well as their thermal properties (volumetric heat capacity, volumetric thermal conductivity, thermal diffusivity). As measure of variability, the coefficient of variation CV was used. The sites vary more in the composition of their constituents than in their thermal properties. 56.25 % of soil content CVs but only 16.6 % of thermal property CV's lie above 25 %.

Furthermore, it was investigated if input parameters like thermal diffusivity differ depending on if the moment of data aggregation is hastened. A t-test was conducted to examine the likeliness of a match of the mean of thermal diffusivity calculated for individual samples and a value that is calculated from means as intermediate result. When values vary strongly at the moment of aggregation, it was more likely that the hypothesis of that the resulting thermal diffusivity value equals the mean value of thermal diffusivity of individual samples could be rejected on the 5-% significance level. This is the case when averaging soil content shares.

These findings indicate that resolving soil constituents on a fine scale is important to accurately model thermal properties. Errors made by those models which assume homogeneous soils over large grid-cells might be significant.

Zusammenfassung

Klima Modelle verwenden zur Simulation von arktischen Szenarien oft Eingangsgrößen aus Messdaten, die früh zu Mittelwerten zusammen gefasst wurden. Dies verursacht eine statistische Unsicherheit, die sich als Fehlerfortpflanzung durch den gesamten Rechenprozess zieht.

Um das Ausmaß dieses Fehler auf die Wärmeeigenschaften festzustellen, wurden auf der Insel Kurungnakh im Delta der Lena, Sibirien/Russland an drei Standorten im Relief Proben genommen. Vergleichbare Böden Horizonte wurden nach der Variabilität des Anteils ihrer physikalischen Bestandteile (Luft, Eis, Organik, Feststoffe, Wasser) sowie thermischen Eigenschaften (volumetrische Wärmekapazität, volumetrische Wärmeleitfähigkeit, Wärmediffusivität) untersucht. Als Maß der Streung wurde der Variationskoeffizient CV verwendet. Dabei hat sich herausgestellt, dass sich die Standorte stärker in ihren physikalischen unterscheiden als in ihren thermischen Eigenschaften. So liegen 56.25 % der CV von Bodenanteile aber nur 16.6 % der CV von thermischen Eigenschaften über 25 %.

Außerdem wurde untersucht, ob sich Eingangsgrößen für Modelle, wie die Wärmediffusivität, verändern, wenn der Moment der Aggregierung vorgezogen wird. Dazu wurde mit einem t-test die Wahrscheinlichkeit berechnet ob der Durchschnitt aus Wärmediffusivitätswerten einzelner Proben mit einem Wert für Wärmediffusivität überein stimmt, der aus Durchschnittswerten als Zwischenergebnis berechnet wurde. Bei einer hohen Streuung der Werte zum Zeitpunkt der Aggregierung konnte auf dem 5-% Signifikanzniveau abgelehnt werden, dass der resultierende Wärmediffusivitätswert mit dem Durchschnittswert aus Wärmediffusivitäten einzelner Proben übereinstimmt. Das ist der Fall wenn über die Bodenanteile gemittelt wird.

Die gewonnen Erkenntnisse legen nahe, dass es wichtig ist physikalische Bodenanteile hochaufzulösen um Wärmeeigenschaften präzise zu modellieren. Die Unschärfe von Modellen, die homogene Böden über große Auflösungsraster annehmen, könnte erheblich sein.

1 Introduction

The role of permafrost degradation and its potential to accelerate climate change has been discussed by scientists for quite some time now (Vincent et al. (2017), Mars and Houseknecht (2007)). Higher temperatures in the arctic tundra have a positive effect on microbiological activity. This enhances the decomposition of soil organic matter (SOM) within the active layer of permafrost-affected soils (Walz et al., 2017).

Permafrost-affected soils are defined as ground that maintains a temperature below 0 °C for more than two consecutive years. This ground can consist of bedrock, sediment, soil or organic matter and may contain ground ice (Grosse et al., 2011). Permafrost-affected soils are further vertically subdivided into an active-layer, which is affected by seasonal thawing, and an underlying frozen-layer, which stays frozen throughout the entire year, even through summer. Of particular significance are the 1,387,000 km^2 (Strauss et al., 2013) of

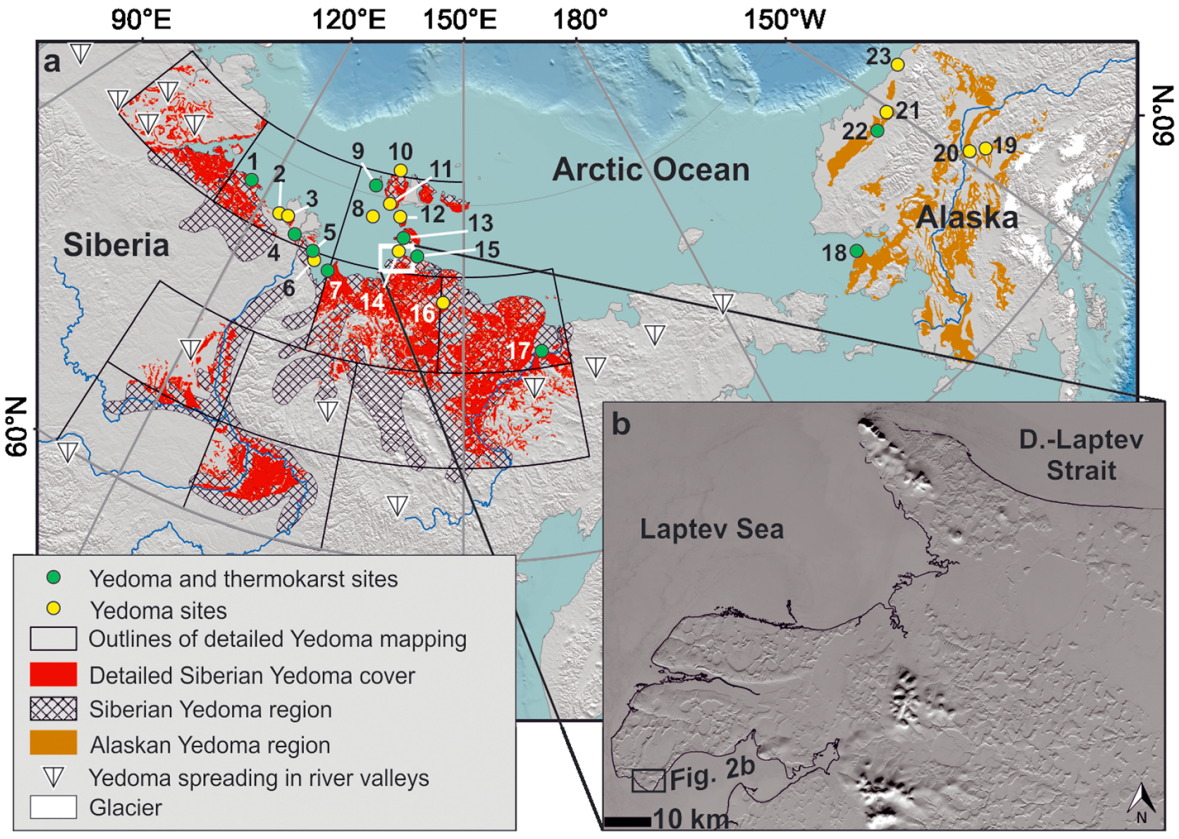

Figure 1: Distribution of Siberian and Alaskan Yedoma regions. Taken from Strauss et al. (2013)

Yedoma Ice-Complex landscapes (see figure 1) of the permafrost region in the Northern Hemisphere that are considered ice-rich in the upper 10 meters (with more than 20 % excess ice content). Those syngenetic, i.e. growing at the pace as the surrounding permafrost table, frozen deposits consist of fine-grained and ice-rich material and are widely distributed in the lowlands of Northeastern Siberia, Alaska and Northwestern Canada. Scientists refer to

those deposits as "Yedoma" or "Ice-Complex" in Siberia and as "muck" in North America (Schirrmeister et al., 2013). These deposits are comprised mainly of silt but also contain a high amount of organic matter. The organic carbon pool of the total Yedoma region that is vulnerable to thawing is estimated to 211 + 160 - 153 Pg organic carbon (Strauss et al., 2013). In areas dominated by polygonal tundra, ice-wedges are forming. Those ice-wedges are the result of the repeated process of frost-cracking of the frozen ground in winter. The cracks fill with snow-melt water in spring which freezes again in winter and forms ice-veins (Schirrmeister et al., 2017).

One broad branch of climate research is based on climate models. It is vital to set these models up in an appropriate way to gain reliable results. For example it is important to choose the right size of the grid-cells in models to simulate how quick and deeply soils thaw. Numerical models use many parameters and depend on reliable input which is based on real measurements. To represent permafrost-affected soils correctly, it is important to evaluate these vital parameters e.g. of thawing. Those parameters reflect for example the soils ability to transfer (thermal conductivity) and store (heat capacity) heat.

This bachelor thesis shall examine the variability of soil properties within the active layer of Yedoma Ice complex with regards to landscape configuration. For this purpose, measurements were conducted on Kurungnak island in the delta of the Lena River. The Lena River Delta is bordering the Laptew Sea in the Northeastern Part of the Russian Federation. This delta consists mainly of holocene and some pleistocene sediments and represents with a size of 32,000 km^2 (Hubberten et al., 2006) the largest delta in the Arctic and one of the largest in the world. About $24.10 \cdot 10^6$ t of sediment is transported by with the river discharge and flows into the Laptev sea each year, more than 70 % of that is attributed to the Lena-Delta (Rachold et al., 2000).

On three specific sites (A,C,D) soil profiles were dug (see figure 2). These sites were chosen in cooperation with another study which examined frozen core samples of deeper levels of permafrost excavated by drilling. At Site B, located near a first-order stream, only frozen core samples were taken, which are not included in this thesis. Samples of comparable horizons were taken to measure relative parameter distribution. The shares of the individual soil constituents were quantified and thermal properties were calculated. Spatial variability is unavoidable but becomes a problem the higher the variability or the smaller the space is. Differences in the landscape need to be identified and characterized to reduce small-scale variability. Hypotheses are accordingly:
(1) *the standard deviation of each soil component (air, ice, organic material, solid material, water), within the comparable layers of all sites, is higher than their respective arithmetic mean.*
It is important to test this variability additionally with the thermal properties because there is no linear dependence between soil composition and thermal properties:
(2) *the standard deviation of thermal properties (heat capacity, thermal conductivity, thermal diffusivity), within the comparable layers of all sites, is higher than their respective arithmetic mean.*
Lastly, it will be investigated if thermal properties of a comparable layer differ depending on how they are calculated: (a) Thermal properties are calculated for each measurement site and then aggregated. (b) measurements of the soil components are first aggregated

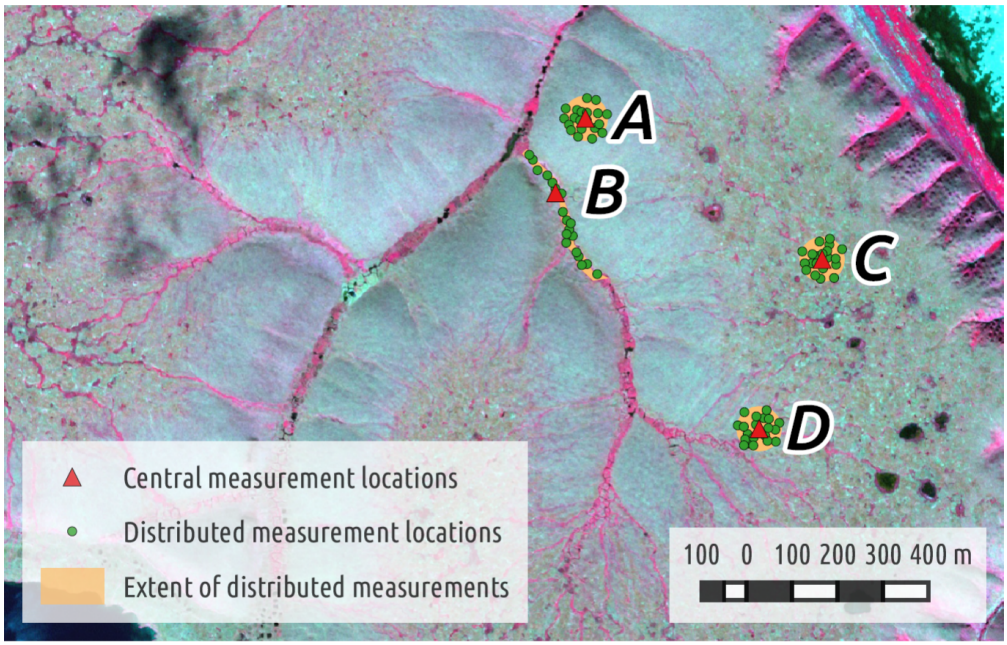

Figure 2: Site A is located on a dry hillslope that is inclined to a first- to second-order stream. Site B is located near a first-order stream in a small valley (not included in this thesis). Site C is located on an upland plateau with mostly undegraded permafrost and small amounts of polygonal-like ponds. Site D is located in an headwater area where water begins to accumulate and flows along small tracks. Adopted from Jan Nitzbon.

and thermal properties are computed later. Many land surface models do not resolve the small-scale variability of soil (thermal) properties but rather use already aggregated data (path b) to reduce computational costs. The possibility of these small-scale errors must be considered and quantified. Therefore:
(3) *the mean values for thermal diffusivity of all locations differ significantly from the values for heat diffusivity calculated from mean values for soil contents.*

2 Methods and Material

2.1 Field work

All of the sampling was carried out in September 2017. The study area on Kurungnakh Island is characterized by an arctic continental climate with a mean annual air temperature is -12.3 °C with a mean monthly temperature of the warmest month (July) recorded as 9.5 °C and for the coldest month (February) as -32.7 °C. The average annual rainfall was 169 mm and the average annual winter snow cover 0.3 m, with a maximum snow depth of 0.8 m recorded in 2017. This meteorological data derives from the record of the Samoylov meteorological station (72° 22' 12.036" N, 126° 28' 51.816" E) on the neighbouring Samoylov Island and dates from 2002 to 2017 (Boike et al., 2018).

The sites A, C and D differ with respect to their topographical features of the studied Yedoma landscape: Site A (72° 22' 6.7908" N, 126° 15' 24.2316" E) is located on a slope, C (72° 21' 57.5928" N, 126° 16' 20.9856" E) is on an upland plateau and D (72° 21' 45.2628" N, 126° 16' 7.8492" E) in an area where water gathers in small tracks that visibly starts to flow. For each site, a central profile with chosen GPS coordinates was declared that was representative for that specific topographical feature in the landscape. Additionally, for further statistical weight, up to 20 supplementary profiles were distributed randomly within a 50 m radius area around each central profile.

For each site, the thaw depth was measured with a stainless steel bar that was plunged into the soil until it hit frozen ground. The position of the top moss layer was marked with a flat hand. After extricating, the before buried part of the bar could then be measured by length. When tussocks, small bunches of grass, were in the way, the leaves were pushed aside and measured from the moss-line. This process was repeated 5 times and a mean value was calculated.

The horizon limits in the central profiles were classified by German "Kartieranleitung 5th Edition" KA5 (Boden, 2006) and the "International Reference Base for Soil Resources" WRB (IUSS Working Group WRB, 2015). To compare horizons with each other, the profiles were subdivided into a peat layer, humus layer, mineral layer and frozen layer with the help of characteristics like soil color, plasticity, density, vegetation and water content.

Two samples of each of the humus- and mineral- layers were cut out with 100 cm^3 core cutter rings for further analysis. First the overlying horizon was carved out with a knife. Then a sampling ring was hammered in with a mallet while a flat piece of wood on top of the ring provides equal distribution of pressure. As soon as the sampling ring was completely buried but has not yet entered the underlying horizon, it was cut out with chunks of the surrounding soil. Before covering with caps on both ends, overhanging material was trimmed. Afterwards the sample was packed into plastic bags. Samples of the frozen- layer were taken out with a Pürckhauer drill. For that, the Pürckhauer was drilled into the frozen ground up to a depth between 5 and 10 cm.

2.2 Lab analysis

The lab analysis was conducted in the AWI laboratory in Potsdam in March 2018. For the grain size distribution analysis, organic matter has to be removed from the sample while it is essential for the C/N ratio and TOC analysis. For that reason, each sample was subdivided into two cups after freeze-drying.

2.2.1 Grain size distribution

To remove the organic content, the sample was put into a beaker, filled up with 3 % H_2O_2. Over a period of 3 weeks, this emulsion was placed on a stirrer. Each day, 10 ml of 30 % H_2O_2 was added to maintain a constantof acidity. For the pH to be in the optimal range of 6.5 to 8, the emulsion was tested afterwards and, if needed, regulated with ammonia (NH_4^+) or acetic acid (CH_3COOH). After all organic matter was dissolved and no visible reaction could be detected, the solid part is separated from the fluid part with a centrifuge and finally freeze-dryed over night. To 1 g of each water-free sample, dispersant ($Na_4O_7P_2 \cdot 10\ H_2O$) and ammonia solution is added until a 250 ml cup is filled to 2/3 of its volume. After at least one night in a rotating shaker, the content of the cup is subdivided between 8 rotating glasses of a funnel. Depending on the similarity of the distribution curve 3 to 8 of the glasses are given into the "Malvern Mastersizer 3000" for a high resolution grain size distribution analysis. The Mastersizer 3000 categorizes 100 grain size bins ranging from 0.01 μm to 3500 μm by optical obscuration of a laser beam.

2.2.2 Element analysis

The samples from the cups for the element analysis were grinded in agate jars with agate grinding balls for 6 to 8 minutes at a maximum milling speed of 360 rpm. Because in some samples, there was only little material left after milling, a clean brush was used to recover most of the sample. A small amount of Wolframoxide (WO_3) was added to 5 mg of each sample, then packed in tin caps, weighted and passed to an automatic element analyser. A second tin cap with higher amounts (15 mg to 70 mg) of the sample, depending on the carbon content, were again packed in tin caps without adding WO_3, weighted and passed to the TOC-Analyser. An overview of the lab results for C, N and TOC is added as a table in the Apendix.

2.3 Computing and statistics

2.3.1 Soil contents

The volumetric content θ_n of each soil constituent is determined by the ratio of its volume V_n to the volume of the sample V_{sample}. The subscript n always refers to the soil constituents air, ice, organic material, solid material, water.

$$\theta_n = \frac{V_n}{V_{sample}} \tag{1}$$

Because samples of humus- and mineral layers are gained by core cutter rings, V_{sample} is a fixed value for those samples. Samples that are retrieved by Pürckhauer driller are of varying length. Their volume not only differs within active layer samples but also within frozen layer samples and needs to be calculated specifically for each sample. The samples are weighted in a wet m_{wet} and dry m_{dry} state, while being boxed in an aluminum container. The difference equals the weight of the contained ice or water. The respective volume $V_{ice,wat}$ is calculated by dividing that difference by its density $\rho_{ice,wat}$. All used densities are also displayed in table 1.

$$V_{ice,wat} = \frac{m_{wet} - m_{dry}}{\rho_{ice,wat}} \tag{2}$$

The total mass of organic matter is calculated by multiplying m_{dry} by the total organic carbon TOC (weight-%) and a factor $hf = 1.724$. This factor, known as humus-factor, originates from an assumed mean carbon content in organic matter of 58 % (Amelung et al., 2018). Divided by its density ρ_{org}, the volume for the containing organic matter V_{org} is calculated.

$$V_{org} = \frac{m_{dry} \cdot TOC \cdot hf}{\rho_{org}} \tag{3}$$

To calculate the Volume of the solid fraction V_{sol}, the previously used organic matter mass is simply subtracted from m_{dry} and divided by the density ρ_{sol}. Since the remaining content in the solid fraction is assumed to consist of mostly quartz, it is reasonable to use the density of quartz in this case.

$$V_{sol} = \frac{m_{dry} \cdot (1 - TOC \cdot hf)}{\rho_{sol}} \tag{4}$$

To calculate the air volume V_{air}, all other fractions are subtracted from V_{total}.

$$V_{total} = V_{air} + V_{ice} + V_{wat} + V_{org} + V_{sol} \tag{5}$$

Since the calculation for the volume of every fraction contains errors and uncertainties it is possible for V_{air} to theoretically result in a negative volume. In this case total water saturation is presumed and for further calculation the air volume is defined as 0.

2.3.2 Volumetric heat capacity

The total volumetric heat capacity c_v in one sample is the sum of the volumetric heat capacities of the individual soil constituents $c_{v,n}$ weighted by their respective volumetric content θ_n. The volumetric heat capacity values used in this thesis are listed in table 1.

$$c_v = \sum_n \theta_n \cdot c_{v,n} \tag{6}$$

2.3.3 Thermal conductivity

Several models exist to calculate the thermal conductivity of soils. The input parameters for the model, developed by Johansen (1975), are easy to obtain. A newer model was developed by Endrizzi et al. (2011). Fröb (2011) shows, that the results of de Vries (1952) are still the

most accurate. In this thesis, only the model of de Vries is used. Adjustments and from Campbell et al. (1994) and Fröb (2011) are applied as described below. First, it is assumed that all soil particles in the solid fraction have a spherical shape (de Vries, 1975). The model was originally developed with an water-air system in mind, meaning that the pores were either filled with water, air or both. Fröb (2011) and Ippisch (2001) both adapt this successfully on an ice-air system by using the same input parameters as for the water-air system. Samples of this thesis are expected to have either an air-water or an air-ice system. For simplification reasons it is assumed that samples from frozen layers do not contain any liquid water. Vice versa, active-layer samples do not contain any ice. To calculate the thermal conductivity K_h of a sample, the thermal conductivity of every soil constituent was used in combination with its volumetric share θ_n and a weighting factor f_n.

$$K_h = \frac{\sum_n f_n \theta_n K_{h,n}}{\sum f_n \theta_n} \tag{7}$$

where $K_{h,n}$ is the conductivity of the soil constituent, f_n the weighting factor and θ_n the constitutents volumetric share as calculated in equation 1. The weighting factors f_n are, to a large extent, determined empirically in the de Vries theory and describe the influence of the respective constituent. Thermal conductivity values for the pure fractions are used as listed in table 1.

$$f_n = \left[1 + \frac{1}{3}\left(\frac{K_{h,n}}{K_c} - 1\right)\right]^{-1} \tag{8}$$

with K_c is the thermal conductivity of the continuous phase that connects all constituents. This phase can only be formed by water, ice or air, as all solid partiles are assumed to be of spherical shape.

$$K_c = K_{h,air} + \beta_{a-w}(K_{h,wet} - K_{h,air}) \tag{9}$$

where β_{a-w} is an empirical weighting function that ranges from 0 for dry soils to 1 for fully saturated soils. $K_{h,air}$ is the thermal conductivity of air. The Index *wet* describes that this parameter is used differently for active-layer and frozen-layer samples. In frozen-layer samples, the parameters with the index *wet* are replaced by their property for *ice*. In active-layers, the pendant for *water* is applied.

$$\beta_{a-w} = \left[1 + \left(\frac{\theta_{wet}}{\theta_{f,0}}\right)^{-\epsilon_s}\right]^{-1}, for\ 0 \notin \theta_{wet} \tag{10}$$

Again, θ_{wet} is replaced by the volumetric content of water in active-layer samples, respectively ice in frozen-layer samples. $\theta_{f,0}$ is a parameter that relates to the water or ice content at which it affects thermal conductivity and the rapidity of transition from air to water or ice-dominated conductivity (see Campbell et al. (1994), P.308). ϵ_s is a smoothing parameter that is specific for different soils. In this thesis, $\theta_{f,0}$ is set to 0.15 and $\epsilon_s = 4$ as used by Fröb (2011) for a study area on Kurunghnak and Samoylov.

2.3.4 Thermal diffusivity

The thermal diffusivity α measures the spatio-temporal heat transfer in a material due to a temperature gradient. It describes how quickly heat moves through a substance because it conducts heat very well relative to its volumetric heat capacity.

$$\alpha = \frac{K_h}{c_v} \tag{11}$$

with c_v and K_h being calculated as in equations 6 and 7.

2.3.5 Arithmetic mean

The arithmetic mean $\overline{x}$ describes the center of a distribution of a set of values resulting from an experiment or an observational study. It is calculated by dividing the sum of the numbers in a set $x_1, x_2, \ldots, x_n$ by their quantity n.

$$\overline{x} = \frac{1}{n}\sum_{i=1}^{n} x_i = \frac{x_1 + x_2 + \cdots + x_n}{n} \tag{12}$$

2.3.6 Standard deviation

To give a perception of the extent of this distribution of values, it is important always to determine the standard deviation σ when calculating a mean. In a Gaussian distribution of values, σ describes the horizontal distance of an inflection point to the maximum. 68 % of measurement data are expected within the area of the two inflection points. σ is defined as the square root of the variance var, which is calculated by summarizing of the squares of the differences of the arithmetic mean $\overline{x}$ to the values in a set $x_1, x_2, \ldots, x_n$ and dividing the result by the quantity minus one.

$$\sigma = \sqrt{var(x)} = \sqrt{\frac{\sum_{i=1}^{n}(x_i - \overline{x})^2}{n-1}} \tag{13}$$

2.3.7 Coefficient of variation

The standard deviation σ is a good indicator to show the spread in a data set. But if two data sets differ in units or dimensions, it can be misleading. To compare such data sets, the coefficient CV can be used which is defined as σ is divided by $\overline{x}$.

$$CV = \frac{s}{\overline{x}} \tag{14}$$

2.3.8 One-sample t-test

The t-test is a very useful tool to compare a calculated mean value of a population to a hypothetical mean. In this thesis the mean of a set of thermal diffusivity values shall be compared to a thermal diffusivity value calculated by means. If both means are the same,

Table 1: Properties of the soil constituents taken from Fröb (2011). [1]properties for quartz apply for the solid fraction as it is assumed to be comprised mostly of quartz.

constituent	c_v $[Wm^{-1}K^{-1}]$	K_h $[MJm^{-3}K^{-1}]$	ρ $[kgm^{-3}]$
air	0.025	$9.26*10^{-4}$	1.2041
ice	2.2	2.0	917
organic	0.3	2.3	1300
solid[1]	2.9	2.4	2650
water	4.17	0.6	1000

it does not matter where data is aggregated in the computing process. Typically a t-test outputs a t-value and a p-value to suggest if the hypothesis should be supported or rejected.

$$t = \frac{\overline{x} - \mu}{\frac{\sigma}{\sqrt{n}}} \tag{15}$$

with $\overline{x}$ being the arithmetic mean as in equation 12, σ the standard deviation as in equation 13 and n the number of values. μ describes the hypothetical mean. If the t-value lies outside of the 95 % range of the expected values, or confidence interval, the hypothetical mean is strange and likely to be different of the compared population. The limits of this confidence interval, or critical values, depend on the level of significance $\alpha = 0.05$ and the degrees of freedom $df = n - 1$. Those values can be taken from the t-distribution tables of two tailed tests in literature such as Sachs and Hedderich (2006). Since the investigated layers in this thesis differ in sample size, the confidence limits differ as well (humus- and mineral-layer $\pm$ 2.5706, frozen-layer of central profiles $\pm$ 4.3027 and frozen-layer of satellite profiles $\pm$ 2.1314). P-values, on the other hand, describe the possibility or likelihood that such an experimental situation (or a more extreme one) occurs while still maintaining the null-hypothesis. If the p-value falls below the level of significance α it can be used as evidence against the credibility of the null-hypothesis within the known parameters of the testing-environment. T-values and p-values can be calculated manually by using equation 15 or the "t.test" command in R (R Core Team, 2018).

3 Results

3.1 Soil profiles

3.1.1 A00 - slope

The soils were classified by German "manual of soil mapping, 5th Ed. (KA5)" (Boden (2006)), are in the following referred as KA5, and "the International soil classification system for naming soils and creating legends for soil maps" IUSS Working Group WRB (2015), further referenced as WRB. To compare different horizons with each other in terms of their composition and thermal properties, horizons were given the additional labels: The surface layer consists of a small seam of living moss on top of dead, slowly decomposing vegetation and/or roots which together forms the highly organic "peat layer". No samples were taken from this layer. The second layer marks a volumetric increase in solid, non-organic material. As the amount of organic matter is still very high, it is called "humus layer". Beneath, a layer is found that has a notably high amount of the silt and fine sands fraction and is further referenced as "mineral layer". The permafrost table marks the current active-layer thickness (ALT) as well as the upper end of the "frozen layer" which is assumed to be completely frozen and contains no liquid water. The lowest investigated layer, determined by motorized drilling, distinguishes itself by a sudden increase of excess ice and a drastic drop in solid material. The analysis of this "ice complex" is beyond the scope of this thesis. Its existence is merely acknowledged by a visual confirmation within 1 m depth. Figure 3 offers a schematic overview of the three sites. Since frozen soils are not considered of in KA5, a trade-off has to be made to determine a soil type by German classification: frozen layers are handled as unfrozen, i.e. the amount of ice acts as water content. Ice wedges on the other hand are only in the WRB system acknowledged. Another difference in classification systems are the measured depths. The limiting values for horizons in the KA5 start from the top of the terrain surface (**GOF**, from German, Geländeoberfläche), the WRB also measures the depth from the mineral soil surface (**MSS**) for some parameters. If not mentioned explicitly, MSS depths are used (also shown in table 2).

Site A was chosen to be representative for a typical slope of a thermo-erosional valley in an otherwise flat Yedoma landscape. In the thawing season, the 9 cm thick peat layer acts like a sponge, soaking rain water and releasing it to deeper levels. The underlying, 14 cm thick $sGo-Ah$ horizon is affected by run-off water. Rusty-red spots are visible and outbalance pale colors of reduction. This is a sign of oxidizing conditions and fluctuation of water content. The narrow C/N ratio (table 2) indicates high humus quality and decomposition. In the neighbouring $Ah-sGo$ horizon, rusty spots decrease in area but do not disappear completely. A darker color points to a higher share of organic content (see figure 4 II). The texture does not vary much among horizons. Most of the time, grains of sand are visible but if not always tactile by hand. Finer grains predominate the solid part. Grain size distribution analysis in

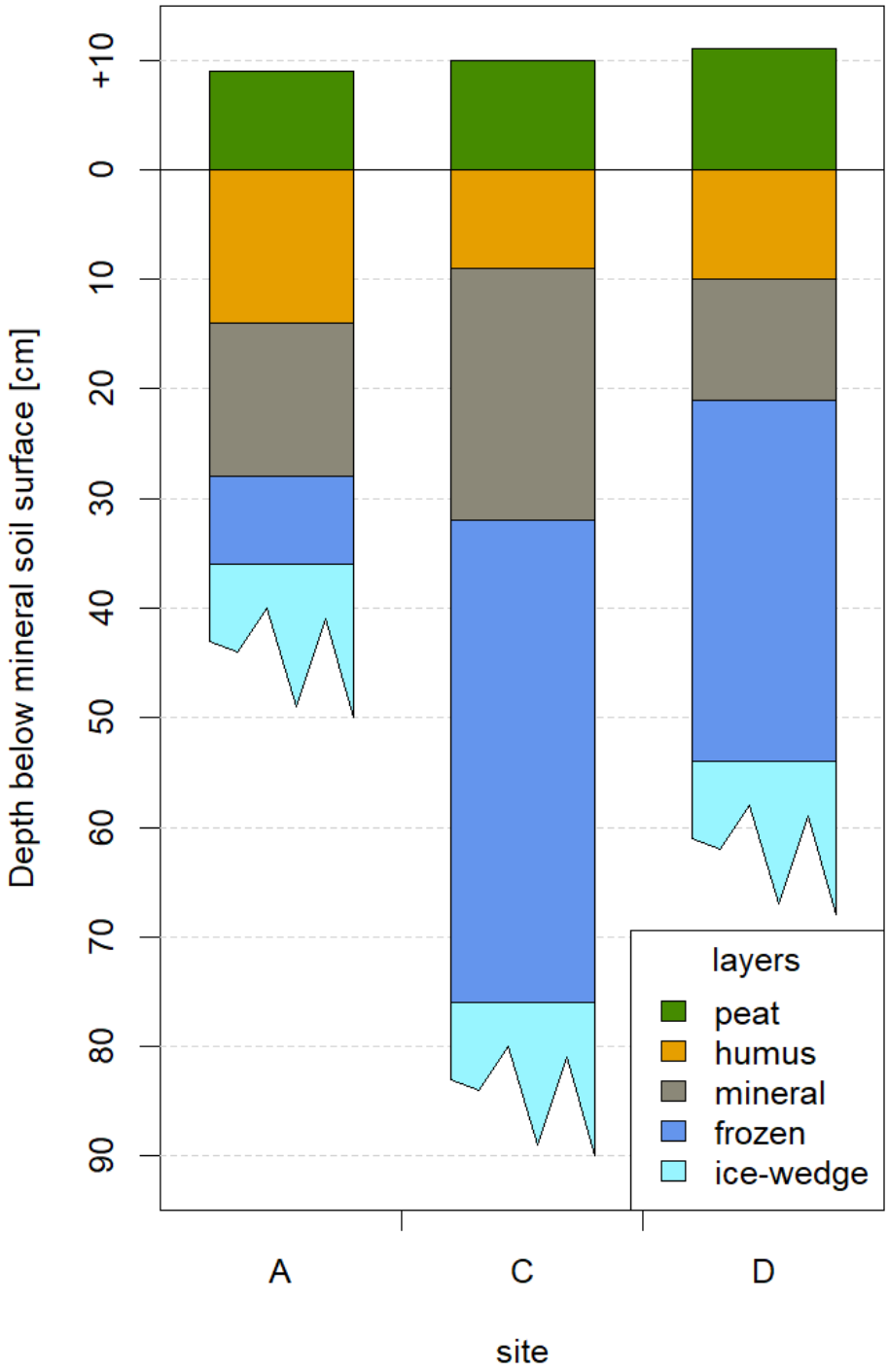

Figure 3: Schematic composition of layers in central profiles on the sites A,C and D.

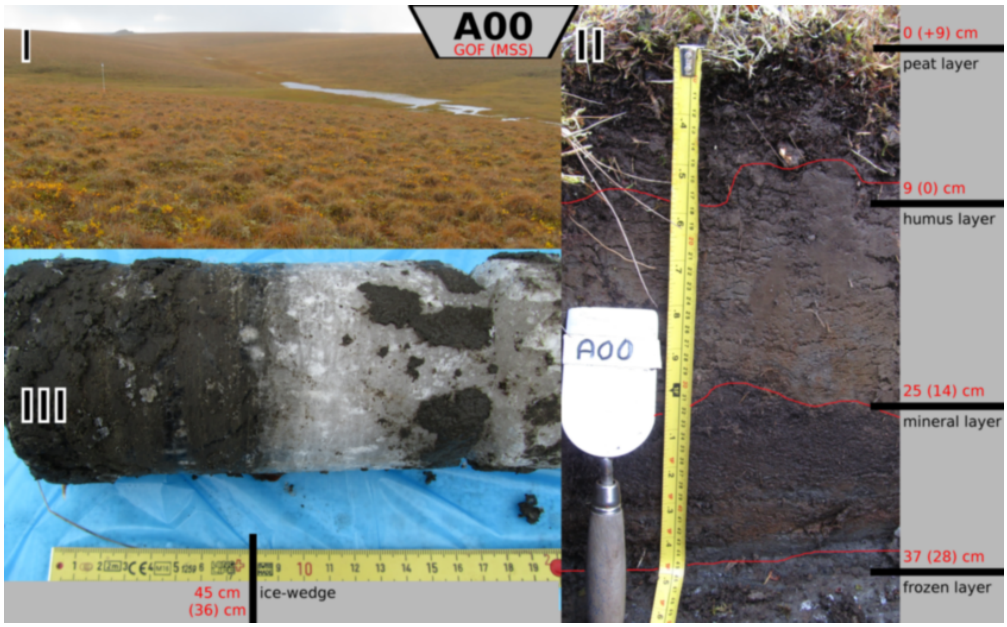

Figure 4: Profile site A, I: intermediate view of the profile surroundings; II active layer profile; III: transition of the frozen layer to ice-wedge visible in the core.

the lab (see tab. 2) confirms the presumption of sandy silt. The prefix s used before capital letters G indicates the influence of slopy run-off water. The $Ah - sGr$ horizon starts within 40 cm GOF which qualifies for a Hangnassgley. To summarize the soil profile:

GNg:ff-su (Fmu, qh)/ff-su(Fmu,qh)/ff-lu(Fmu,qh).

The diagnostic cryic horizon for a Cryosol starts at 28 cm depth. A lower mineral content gives space to air and excess-ice. A drilling core marks the start of the ice-wedge at 36 cm depth. On base of the lab analysis of the ice-content in the frozen layer, it is visibly reasonable to assume the ice-wedge contains more than 75 % excess-ice, which is also the condition for a principal qualifer of "glacic". The subqualifier "kato" means that the cryic horizon starts within 50 cm of the mineral soil surface and does not end before 100 cm depth. Furthermore the supplementary qualifier "profundihumic" applies since, up to a depth of 100 cm below mineral soil surface, the weighted mean of organic carbon is above 1.5 %. By classification of WRB this site is considered as a

Katoglacic Cryosol (Profundihumic).

3.1.2 C00 - plateau

The $Go - Ah$ horizon in the central profile of site C starts 10 cm under a layer of peat. A organic matter content of 20.43 % implies extrem-humicity. By increasing depth, total organic content (TOC) falls rapidly but stays above a weighted mean of 3.05 % organic carbon (Profundihumic). Because of the high organic content, the horizon could be considered *Aa* for half-boggy (from German, anmoorig). Although there is no information about the acidity level available and the low C/N ratio (table 2) of below 15 suggests an unusual high decomposition for *Aa* horizons. A theoretical negative air content was caluclated for the 9 cm thick $Go - Ah$ horizon as well as the underlying $Ah - Go$ horizon. This highly suggests total saturation of water content. Due to the location on a upland plateau (see figure 5), water

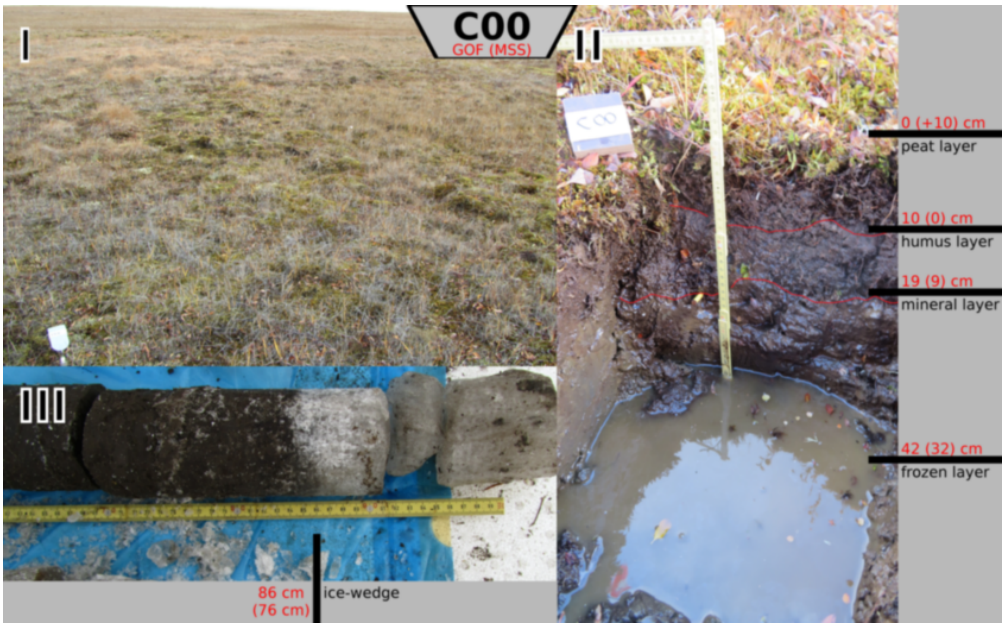

Figure 5: Profile site C, I: intermediate view of the profile surroundings; II active layer profile; III: transition of the frozen layer to ice-wedge visible in the core.

run-off is considered generally weak which indicates a water saturation for the thawing season for more than 30 consecutive days in the humus- and mineral layer (Epihistic). In contrast to the overlying layer, the $Ah - Gr$ horizon contains a much higher mineral content of 56.26 %. The C/N ratio increases slightly which indicates lower decomposition. Some reddish spots are still visible in the pale $Ah - Gr$ whereas the frozen Gr only reveals reduction colors. Due to the upper boundary of the Gr horizon in a depth of 42 cm below GOF, the pale color palette and the high decomposition, this soil profile can not be of the type Anmoorgley but must be classified as Humusnassgley:

GNh:ff-lu(Fmu,qh)/ff-su(Fmu,qh)/ff-lu(Fmu,qh).

Under the permafrost table of 33 cm below mineral soil surface, volumetric water content in form of ice increases again. The ice-wedge was found by drilling to be starting in a depth of 77 cm (Endoglacic). By WRB classification, this is considered

Epihistic, Endoglacic Cryosol (Profundihumic).

3.1.3 D00 - water tracks

The peat layer above the humus layer in the central profile of site D ends in 11 cm depth below GOF. This is were the Hw horizon starts which contains more than 30 (mass-)% organic matter and is considered above 90 % water saturated (Epihistic). In the underlying Ghr-horizon, the content of organic matter falls on 4.99 %. The color palette of the horizon (clearly visible in figure 6) implies reductive conditions. A C/N ratio as high as 20.7 indicates a bog-like low decomposition grade. By KA5 classification, this soil profile is considered a Moorgley:

GH:ff-lu(Fmu,qh)/ff-su(Fmu,qh)/ff-lu(Fmu,qh)

The silt-dominated Ghr horizon starts in a depth below mineral soil surface of 21 cm and is thicker than 30 cm (Siltic). The TOC-content drops only to 2.83 % which makes a 100 cm

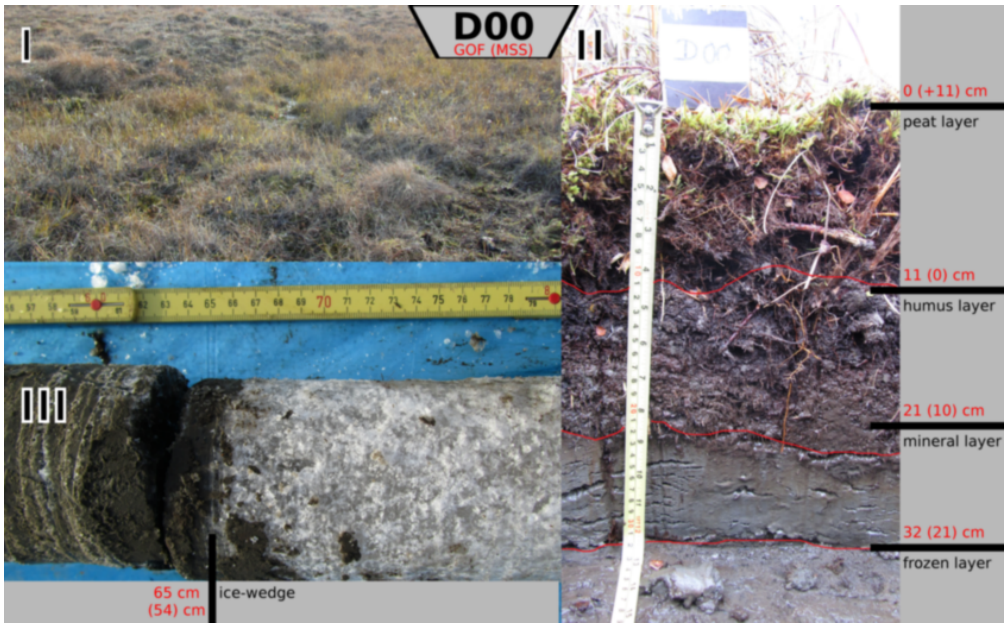

Figure 6: Profile site D, I: intermediate view of the profile surroundings; II active layer profile; III: transition of the frozen layer to ice-wedge visible in the core.

weighted mean of 5.99 % organic carbon (Hyperhumic). Finally, the ice-wedge in 55 cm depth below mineral soil surface qualifies for a

Epihistic, Endoglacic Cryosol (Siltic, Hyperhumic).

3.2 Variability of soil components

The shares of components θ_n in the composition of soil layer within each profil vary with depth (see fig. 7 **(a)**). The n index stands for the components air, ice, solid, organic, water. The mineral layers of profiles A and D hold with a maximum share of about 2 % very little air. Both neighbouring layers are with an θ_{air} of at least 10 % much better ventilated. Since θ_{air} is calculated as the difference of all other components to 100 %, negative values are theoretically possible and handled as an assumed maximum water saturation. This is the case for the humus- and mineral layer of the central profile at site C. For all further computing, an θ_{air} of 0 % is applied. The humus layer of profile C simultaneously represents the highest share of water with a θ_{water} of over 80 %. The lowest θ_{water} in a mineral layer is found in profile D which is located in the water-tracks area. However, in the humus layer directly on top of that, the θ_{water} is still above 70 %. It is assumed that no water in frozen state occurs in the active layers just as no fluid water occurs in frozen layers. All frozen layers hold an θ_{ice} of above 50 %. All active layers show an $\theta_{organic}$ of over 5 % with one exception of the humus layer (4.37 %) of the central profile at site A (slope). The highest amounts of organic content with over 8 % is found in the humus layer of the central profile at site D (water tracks). θ_{solid} orientate strongly anti-proportional with water respectively ice contents. The higher the amount of water in a sample, the smaller the share of solid content.

In a horizontal comparison of the soil components (see fig. 7 **(a)**) within their comparable layers, only one mean value (in specific: the θ_{air} of humus layers) is higher than its respective

Table 2: Soil properties of central profiles and frozen layers of satellite profiles.

Site ID	# of samples	depth [cm]	horizon KA5	comparable layer	TOC [%]	SOM [%]	C/N ratio	texture Clay	Silt	Sand
A	0	+9 - 0	O	peat						
	2	0 - 14	sGO-Ah	humus	4.03	6.94	14.57	7.64	62.68	29.68
	2	14 - 28	Ah-sGO	mineral	4.75	8.18	14.23	7.9	65.14	26.96
	1	28 - 36	Ah-sGr	frozen	4.72	8.14	14.57	8.94	64.98	26.08
	0	36 - ??		ice-wedge						
C	0	+10 - 0	H	peat						
	2	00 - 9	Go-Ah	humus	11.85	20.43	14.67	8.41	64.33	27.26
	2	9 - 32	Ah-Gr	mineral	3.05	5.26	18.47	7.98	73.38	18.63
	1	32 -76	Gr	frozen	2.24	3.86	19.42	11.19	72.13	16.86
	0	76 - ??		ice-wedge						
	10	30.9	Gr	frozen (sat.)	2.24	7.55	19.42	9.25	66.91	23.84
D	0	+11 - 0	H	peat						
	2	0 - 10	Hw	humus	18.58	32.04	14.57	8.69	71.11	20.2
	2	10 - 21	Ghr	mineral	2.9	4.99	20.7	7.1	70.5	22.4
	1	21 - 54	Ghr	frozen	2.82	4.86	16.27	10	68.15	21.84
	0	54 - ??		ice-wedge						
	6	29	Gr	frozen (sat.)	2.24	9.28	19.42	8.05	68.71	23.25

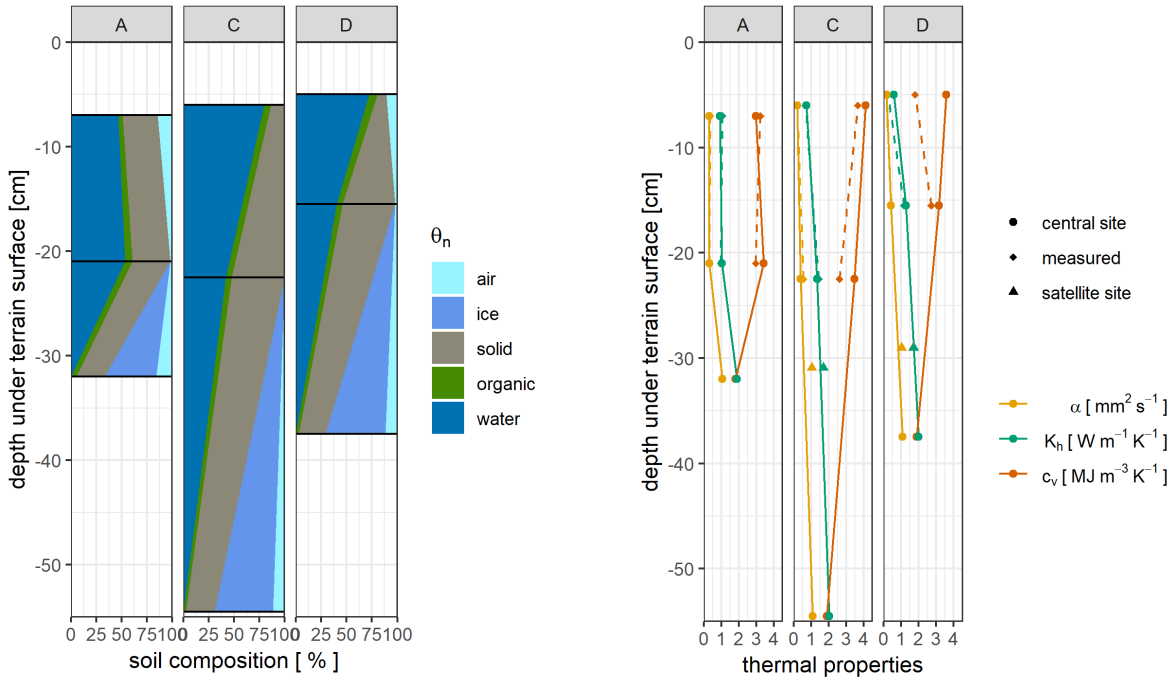

(a) Soil composition **(b)** Thermal properties

Figure 7: Distribution of **(a)** soil constituents and **(b)** thermal properties in central profiles A,C and D. horizontal black bars mark sampling depths. Shapes depict additionally instrument-measured values in active layers of the central profiles as well as calculated values of satellite profiles.

standard deviation σ error. The variation of θ_{air} decreases with lower layers. While the humus layer holds a coefficient of variation (CV) of above 1.3, it is lower than 0.25 in the frozen layer in central profiles. Variation of air contents of the frozen layer in satellite profiles are found in between with a CV of 0.39. The group of water (in active layers) and ice (in frozen layers) contents represent the lowest CV-values. Their highest variation is found in humus layers with a CV of 0.25. A slightly higher variation of soil components shares can be found in the organic content. While frozen layers in central profiles provide the highest CV-value (0.44) within their component group, mineral layers have a CV of only 0.10. Mineral content varies in humus layers with 0.79 much more than in frozen layers (0.04) which is the smallest CV value of soil components at the same time.

3.3 Variability of thermal properties

On the base of the distribution of soil components shown in section 3.2, thermal properties can be calculated for the investigated soils. For that, volumetric heat capacity c_v and thermal conductivity K_h are both determined by summarizing the share of each soil component (see equation 6 and 7). The ratio of K_h to c_v creates a value that describes the spatiotemporal diffusion for heat due to a gradient of temperature: the thermal diffusivity α. In active layer horizons, c_v and K_h are measured additionally in-field by instrument to archive reference values. The measurement, however, requires non-frozen soil. Therefore no measured data

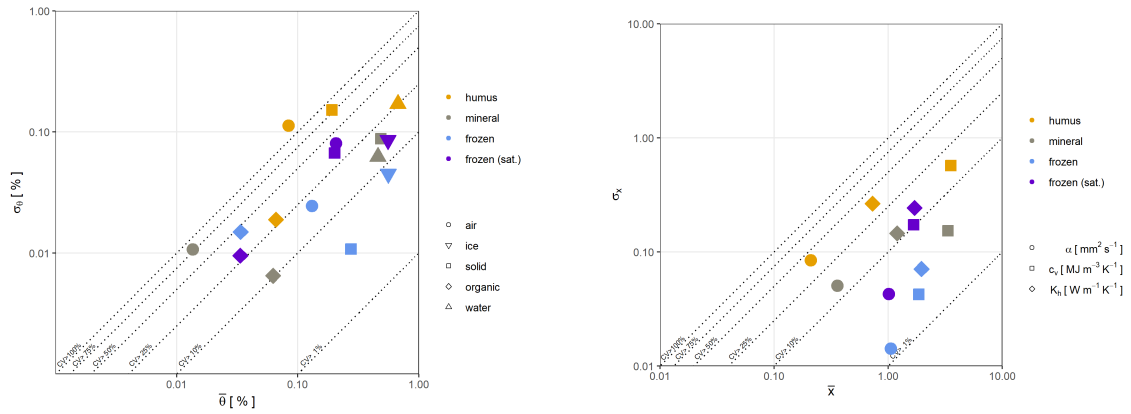

(a) Physical properties **(b)** Thermal properties

Figure 8: Standard deviation σ and mean values of **(a)** soil constituents and **(b)** thermal properties on logarithmic scales. Dotted lines mark noticeable CV values.

could be obtained from frozen layers of central- and satellite profiles. The values for satellite profiles depicted in figure 7 **(b)** derive from calculating sample data.

Profile A is the only site where c_v is higher in the mineral layer than in the humus layer. In the profiles C and D, c_v decreases strictly monotone. The highest value for c_v ($4.1\,\mathrm{MJm^{-3}K^{-1}}$) in central profiles is calculated for the humus layer of profile C, the lowest ($1.81\,\mathrm{MJm^{-3}K^{-1}}$) is found in the frozen layer of profile A though mean values of satellite profiles are even lower.

In contrast to c_v, K_h rises with increasing depth to its highest value within the profile of all sites in the frozen layer. The overall maximum is found in site C: $2.01\,\mathrm{W^{-1}K^{-1}}$). Humus layers contain the lowest values with $0.57\,\mathrm{Wm^{-1}K^{-1}}$ in site D as the overall minimum. K_h values in frozen layers of satellite profiles line up with their respective central profiles almost perfectly by depth.

In the denominator of the α quotient, c_v drops considerably more than K_h is rising in the nominator. As a result, α is strongly increasing with depth throughout all sites. Profile D offers both the overall minimum ($0.16\,\mathrm{mm^2s^{-1}}$) as well as the highest range. Because of the units used to display data in figure 7 (b), c_v and K_h values of frozen layers central- and satellite profiles are hardly distinguishable. This results in a nominal value of α close to 1 with the maximum ($1.07\,\mathrm{mm^2s^{-1}}$) found in the frozen layer of profile C. K_h reference values from in-field measurements in the active layer overlap very good with the calculated data. Measured c_v values only serve as good signposts for trends in calculated data in profile C.

In contrast to the shares of soil components, thermal properties don't vary as strongly within their comparable layers (see fig. 8 **(b)**). Not a single standard deviation error $\overline{x}$ is higher than its respective mean value $\sigma_{\overline{x}}$. The highest distribution of thermal property values is found in humus layers (c_v at 0.16, K_h at 0.36 and α at 0.4). With lower layer depth, variation also diminishes. The lowest CV-values are found in the frozen layers of the central profiles. CV-values of frozen layers in satellite profiles are similar to mineral layer in central profiles.

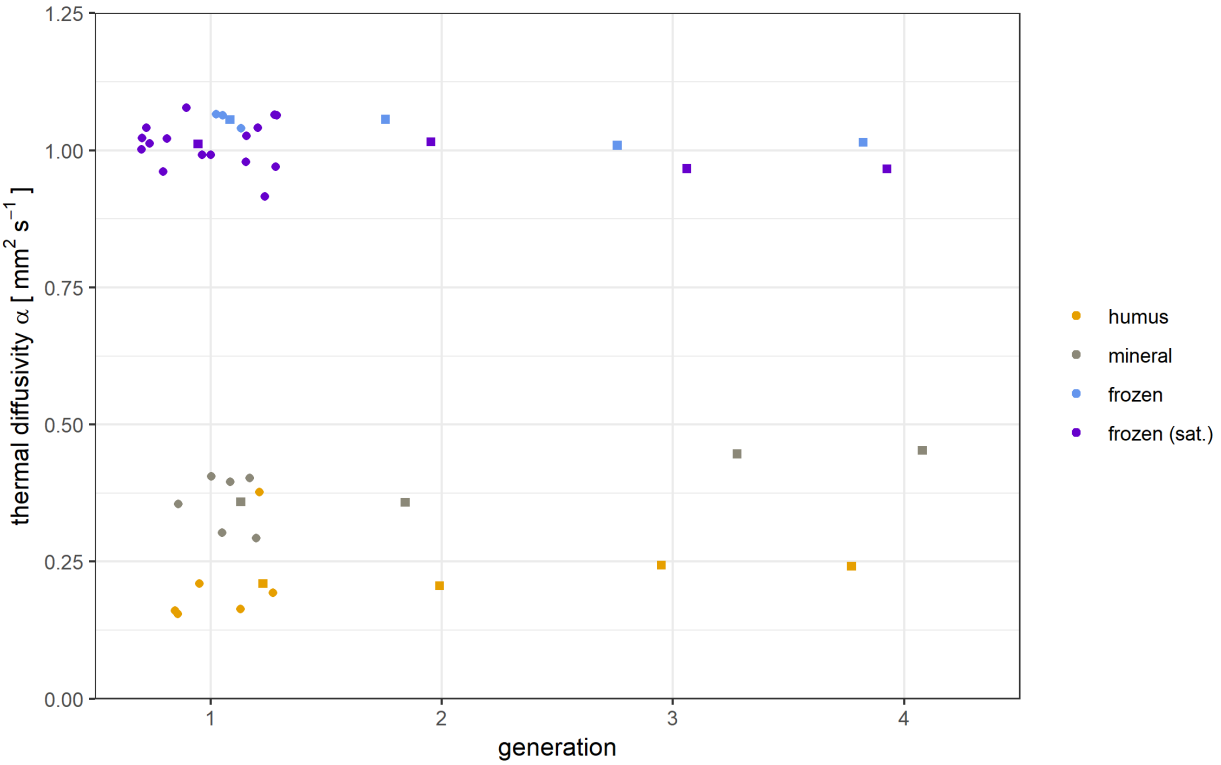

Figure 9: Difference in processing sample data. Generations represent where in the computing process the mean values (squared shaped) were calculated. Jittered dots in the first generation are actual sample data.

3.4 Difference in calculating diffusivity values

When data is prepared to work as input parameters in models, the best-practice is always to prepare as much data as possible beforehand to keep processing power and time on a low level. Parameters like thermal diffusivity α of a specific soil type are, by itself, calculated in a long and elaborate process. So it is captivating to determine an early mean value. Figure 9 shows the difference of α_i in taking means in earlier "generations" of the computation process. The term generation describes a certain step in the computation process where it could make sense to aggregate data and proceed with only one value for a set of samples. In generation 1, α_1 is calculated for every taken sample and subsequently a mean value is formed that can be used as input parameter. In generation 2, mean values are calculated for K_h and c_v which together form α_2 (see equation 11). In generation 3, means are taken from the shares of the soil constituents θ_n. Lastly, in the 4. generation, means are formed of in-field measurements and direct lab-data like wet- and dry weight of the soil sample, TOC content and volume of the core cutter (and Pürckhauer samples for frozen layers respectively).

The individual layers keep their values in their arranged environment in all generations. Meaning thermal diffusivity α is always lower in humus layers than in mineral layers and so on. To be able to reliably tell the difference of α_i values, a t-test has been conducted. The null-hypothesis is that the α values of the samples in generation 1 form a mean that is not different to the α value of generation 2, 3 and 4 respectively. P-values describe the probability that such situations (or more extreme ones) occur while maintaining the null-hypothesis.

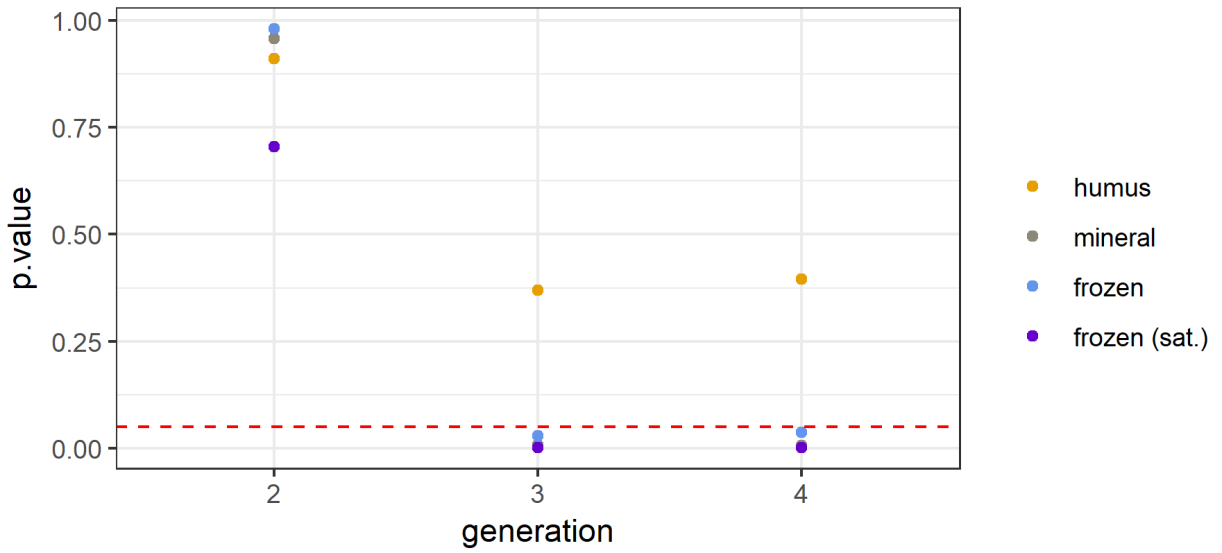

Figure 10: P-values of the t-test. The dotted, red line represents the significance level of 0.05.

Comparable results are shown in figure 10.

In generation 3 and 4, p-values drop drastically and (except for the humus layer) fall below the level of significance of 0.05. It can be concluded that the thermal diffusivity α of those generations and layers are significantly different from the means of their respective samples in generation 1. This is plausible because p-values below 0.05 offer justified doubts of the likelihood that the null-hypothesis applies. In other words, values which are aggregated earlier in the process of calculating input parameters for models and values which are aggregated in the end of the calculation process are significantly different from each other in terms of statistical evidence.

4 Discussion

4.1 Soil layers

What is labeled "humus layers" in this thesis, is classified after the German classification system KA5 as *sGO-Ah* horizon in site A, *Go-Ah* horizon in site C and *Hw* horizon in site D. Other works, such as Walz et al. (2017), define layers comparable to these as bottom active layer. Above lies only a layer mostly comprised of dead vegetation, roots, peat and a fine film of living vegetation, which represents the surface active layer and was not analyzed in this thesis. Both surface and bottom active layers thaw every year. "Mineral layers" can only be accessed by plants when thawed but this deeper layer thaws only in some years. As a consequence there is usually less organic matter and a higher solid fraction in soil constituents than in the upper layer. This is also known as transition zone. Mineral and frozen layer differ mainly in the fact that the frozen layer is frozen at the moment of sampling. A part of the frozen layer or all of it might become part of the mineral layer in other years because the exact thaw depth varies from year to year. This thaw depth marks the boundary between mineral and frozen layer. As ice and water have different thermal properties, the differentiation is important in this work. Literature defines this frozen layer sometimes as permafrost which "presumably not thawed for several decades to centuries" (Walz et al., 2017).

4.2 Classification of soil profiles

The German classification system "Kartieranleitung 5th edition" KA5 does not include frozen soils. It was not developed for soils in arctic latitudes but offers good advice in Gley-soils which are affected by reducing conditions because of groundwater fluctuations which are present in the study area. The "International World Reference Base for Soil Resources" WRB allowes for transfering from different classification systems and includes frozen soils. KA5 differentiates the investigated soils by slope dynamics in Hangnassgley and by humus content in Humusnassgley and Moorgley. WRB, on the other hand, utilizes the underlying ice wedge and the frozen layer to differentiate cryosols. Together, they should provide a good understanding of underlying processes and dynamics in the soil.

4.3 Variability of soil constituents

Site A features only a narrow frozen layer and a high ice wedge which is probably due to the slope dynamics. A high amount of run-off water transports organic and solid material downhill and therefore grind the permafrost table down. Thaw depths vary overall strongly depending on overlaying vegetation and water content. Differences on a small scale were observed but have not been been sampled during the campaign. For example: the active

layer is thicker under tussocks grasses than under a moss cover.

Site C lies on a plane plateau. Water has only little chance to run off and accumulates. Mineral layers generally have less air than frozen layers. This is due to a degrading frozen layer which originally had a higher pore volume. The soil subsides after thawing. Roots usually do not penetrate into a layer which is only sporadically thawed.

The mineral layer of site D has a very siltic composition which tends to block water from tickling down further. Although in the water tracks area, a high water content is prevalent in the humus layer at this site. Most of the water flows within small gullies and the samples were not directly taken from these channels. This is why the velocity is very low and water accumulates similar to site C. The strongest flow of run-off water is presumably in site A which leads to water being immediately drained and causes site A to be the driest o the investigated sites.

The high amount of organic matter in the humus layerof site D is caused by a healthy vegetation that is supported by flowing fresh water and a surplus of incoming nutrients.

Air in humus layers vary strongly (CV>100 %) between sites because of water table dynamics. In contrast, air in frozen layers is very similar in all sites because ice pores have the same elementary structure.

The organic coefficients of variation in figure 8 **(a)** form a cluster of low value, low error. A lower gradient of organic matter in site A causes a higher CV of the humus- and frozen layer within the organic cluster. Although, a high CV values of organic matter suggest a limited comparability as humus layer hardly by any means. A better comparability by organic means would result in a lower CV value for this data point.

In the CV cluster of the solid fraction, the dispersion of values within the layer narrows with increasing depth. While all layers provide for a rather high mean, the spread of values to create this value is much higher in upper layers than in lower layers. This is due to the high variability in the water content in upper layers. Sites that show a high share of the solid fraction (like site A) leave no space for water and exhibit a rather dry state.

4.4 Variability of thermal properties

The volumetric heat capacity c_v is mostly receding with depth caused by a higher share of water in upper levels. Water has a high volumetric heat capacity (see table 1). This is also the reason of the slow rise of c_v in the mineral layer of site A. Water has the highest c_v of the constituents and the value for the c_v of the layer is dominated by the high amount of water in it. Water is eventually replaced by ice in frozen layers with a c_v only half as large as the c_v of water.

In case of the volumetric thermal conductivity, K_h behaves anti-proportional to c_v with increasing depth but for similar reasons. When water is replaced by ice in the frozen layer, a higher K_h applies because $K_{h,ice} > K_{h,water}$. The K_h of ice is also closer to that of the solid fraction which is why the mineral layer represents an intermediate state between the humus layer and the frozen layer. The values of frozen layers ($1.96\,\mathrm{Wm^{-1}K^{-1}}$) are similar to what other works found. The thermal conductivity values of a core on Kurungnakh island of Fröb (2011) range between 2.0 and $2.5\,\mathrm{Wm^{-1}K^{-1}}$.

Since both c_v and K_h highly depend of the amount of ice and water in the layer, their quotient α also depend on the same. Site D features the highest amount of water in the humus layer as well as the highest amount of ice in the frozen layer. Consequently the highest rise of α is also found in site D.

Air performs as a good thermal isolater because of its poor ability to store and conduct heat. Its high variability in humus layers leads further to a high variability in thermal properties. In deeper layers, the values for thermal properties congregate which causes a drop in variability.

The frozen layer is dominated by the ice and solid fraction which feature similar values of c_v and K_h. This causes α to approach 1 ans varies less between sites. Compared to the frozen layers, where no fluid water means lower variability, the humus layers vary more strongly because of the higher difference of thermal properties of the solid fraction to water instead of ice. The mineral layer represents, again, an intermediate state of higher content of the solid fraction and less water.

4.5 Variability of calculation

The difference in calculating α comes into effect when rejuvenating the data aggregation. It really highlights the possibility of a different outcome if data is aggregated in a different stage of the calculation process.

In the t-test, a probability is calculated of how likely a mean of 1st generation α values is similar to a value that is computed of aggregated data. The drop of p-values in the third generation (data is aggregated over θ_n) is caused by a high variability of the content fractions. Compared to the lower overall variability of thermal properties, p-values in the second generation (data is aggregated over c_v and K_h) offer a consequently higher likeliness. It becomes clear that a mismatch to the first generation starts to be apparent in the third generation when averaging over θ_n since 56.25 % of CV are above 25 % and 87.5 % of CV are above 10 %. In contrast to thermal properties where only 16.6 % of CV are above 25 % and 58.3 % of CV are above 10 %. The overall higher variability of content fraction shares over thermal properties already implies a higher uncertainty of correct endresults for α.

Similar results as from third generation α values are shown in the t-test with fourth generation values. Here, data is aggregated over dry- and wet-weight of the sample as well as the sample volume and the TOC content. An outlier value in the humus layer is probably caused by a conspicuous strong weight difference of the samples in site A. This causes a high difference of the solid fraction and the air content (28 %) within the two samples of the humus layer of site A.

5 Conclusion

Accurate input parameters for arctic climate models are crucial to be able to simulate realistic scenarios. Highly aggregated data as input saves processing power and time but increasing uncertainty in inputs values inevitably leads to rather ambiguous outputs.

This thesis surveyed the variability of the share of soil constituents and thermal soil properties of permafrost-affected soils in arctic Yedoma landscapes as well as the calculation process itself. For that, the coefficient of variation for every constituent fraction and thermal property serves as variability measurement. The results show that the investigated physical properties spread more than thermal soil properties. A trend of reducing variability with increasing depth is apparent in both shares of soil constituents and thermal properties. Small scale errors carry weight especially in modelling surface processes like land-atmosphere exchanges.

When calculating thermal diffusivity α, a difference in outcome could be observed, depending of when in the computing process, the data is aggregated. The error really catches attention when aggregating data with high uncertainties due to a high variability of base-values such as volumetric content fraction θ_n or sample specific pre-data from in-field measurements. Although, since thermal properties vary not as much as shares of physical soil constituents, this suggests "processing first, aggregating later" is rather beneficial to keep overall erros for deeper levels low.

Since thermal properties highly depend on the shares of soil constituents, it is important to keep a low variability of soil constituents. Aggregated data can only be used as input parameters for models when the gridcell sizes are chosen in a way to represent data homogeneously. The World Reference Base for Soil Ressources WRB offers a classifications of soils with good indicators of how and where water and ice occurs. High variabilities, especially in upper layers, advocate for smaller gridcell sizes in the investigated area of the Lena River Delta to suit for the high variability in soils and soil properties.

Acknowledgments

This thesis would not have been possible without the help of many people. At this point, I would like to thank ...

... Prof. Lars Kutzbach for supervising me and for actively supporting my scientific career. As a Professor and Mentor, he fostered my curiosity in science and sharpened my critical thinking.

... Dr. Julia Boike for making this whole thesis possible, the outstanding in-field advice, the help with taking the samples and your encouragement in the first place.

... Dr. Norman Rüggen, Dr. David Holl and all colleagues of the AG: Böden im Klimasystem for the interesting and helpful discussions and support in technical and organizational matters.

... Jan Nitzbon for the helpful guidance along the thesis and the long but clarifying e-mails as well as Dyke Scheidemann and the laboratory crew of the AWI in Potsdam for the help of measuring my samples.

... Zoé Rehder and all of my friends for proofreading, tolerating the social neglect and putting up with the whole misery of a thesis-writing student.

... my parents, my brother, my sister and my brother-in-law for morally supporting and motivating me during the whole writing process as well as my niece and two nephews for all the happy faces, sounds and symbols that kept me going.

... and last but not least, I thank you, dear reader, for reading through this undergraduate thesis, for your interest in educational science and checking for your place in the acknowledgement section. You are thanked!

Bibliography

Amelung, W., Blume, H.-P., Fleige, H., Horn, R., Kandeler, E., Kögel-Knabner, I., Kretzschmar, R., Stahr, K., and Wilke, B.-M. (2018). *Scheffer/Schachtschabel Lehrbuch der Bodenkunde*. Springer Spektrum, Stuttgart.

Boden, H. W. E. R. H. S. W. G. K.-J. H. R. H. P. J. H. J. D. K. K.-J. S. R. T. H. A.-h.-A., editor (2006). *Bodenkundliche Kartieranleitung. KA5*. Schweizerbart Science Publishers, Stuttgart, Germany.

Boike, J., Nitzbon, J., Anders, K., Grigoriev, M., Bolshiyanov, D., Langer, M., Lange, S., Bornemann, N., Morgenstern, A., Schreiber, P., Wille, C., Chadburn, S., Gouttevin, I., and Kutzbach, L. (2018). A 16-year record (2002–2017) of permafrost, active layer, and meteorological conditions at the Samoylov Island Arctic permafrost research site, Lena River Delta, northern Siberia: an opportunity to validate remote sensing data and land surface, snow, and . *Earth System Science Data Discussions*, pages 1–77.

Campbell, G. S., Jungbauer Jr, J. D., Bidlake, W. R., and Hungerford, R. D. (1994). Predicting the effect of temperature on soil thermal conductivity.

de Vries, D. (1975). Heat transfer in soils. pages 5–28.

Endrizzi, S., Quinton, W. L., and Marsh, P. (2011). Modelling the spatial pattern of ground thaw in a small basin in the arctic tundra. *The Cryosphere Discussions*, 5(1):367–400.

Fröb, K. (2011). Measuring and modeling of soil thermal properties and ground heat flux at two different sites at Lena Delta, Siberia. Diplomarbeit, Universität Leipzig.

Grosse, G., Romanovsky, V., Jorgenson, T., Anthony, K. W., Brown, J., and Overduin, P. P. (2011). Vulnerability and feedbacks of permafrost to climate change. *Eos*, 92(9):73–74.

Hubberten, H. W., Wagner, D., Pfeiffer, E. M., Boike, J., and Gukov, A. Y. (2006). The Russian-German research station Samoylov, Lena Delta – A keysite for polar research in the Siberian Arctic. *Polarforschung*, 73(2/3):111–116.

Ippisch, O. (2001). *Coupled transport in natural porous media.* PhD thesis, Rupertus Carola University of Heidelberg.

IUSS Working Group WRB (2015). *International soil classification system for naming soils and creating legends for soil maps.*, volume World Soil.

Johansen, O. (1975). *Thermal Conductivity of Soils*. PhD thesis, Institutt for kjoleteknikk 703.

Mars, J. C. and Houseknecht, D. W. (2007). Quantitative remote sensing study indicates doubling of coastal erosion rate in past 50 yr along a segment of the Arctic coast of Alaska. *Geology*, 35(7):583–586.

R Core Team (2018). *R: A Language and Environment for Statistical Computing*. R Foundation for Statistical Computing, Vienna, Austria.

Rachold, V., Grigoriev, M. N., Are, F. E., Solomon, S., Reimnitz, E., Kassens, H., and Antonow, M. (2000). Coastal erosion vs riverline sediment discharge in the Arctic shelfx seas. *International Journal of Earth Sciences*, 89(3):450–459.

Sachs, L. and Hedderich, J. (2006). *Angewandte Statistik: Methodensammlung mit R*. Springer Berlin Heidelberg.

Schirrmeister, L., Froese, D., Tumskoy, V., Grosse, G., and Wetterich, S. (2013). Yedoma: Late pleistocene ice-rich syngenetic permafrost of beringia. In *Encyclopedia of Quaternary Science*, volume 3, pages 542–552. Elsevier B.V., 2 edition.

Schirrmeister, L., Schwamborn, G., Overduin, P. P., Strauss, J., Fuchs, M. C., Grigoriev, M., Yakshina, I., Rethemeyer, J., Dietze, E., and Wetterich, S. (2017). Yedoma Ice Complex of the Buor Khaya Peninsula (southern Laptev Sea). *Biogeosciences*, 14(5):1261–1283.

Strauss, J., Schirrmeister, L., Grosse, G., Wetterich, S., Ulrich, M., Herzschuh, U., and Hubberten, H. W. (2013). The deep permafrost carbon pool of the Yedoma region in Siberia and Alaska. *Geophysical Research Letters*, 40(23):6165–6170.

Vincent, W. F., Lemay, M., and Allard, M. (2017). Arctic permafrost landscapes in transition: towards an integrated Earth system approach. *Arctic Science*, 3(2):39–64.

Walz, J., Knoblauch, C., Böhme, L., and Pfeiffer, E. M. (2017). Regulation of soil organic matter decomposition in permafrost-affected Siberian tundra soils - Impact of oxygen availability, freezing and thawing, temperature, and labile organic matter. *Soil Biology and Biochemistry*, 110:34–43.

Apendix

- In-field data site A.
- In-field data site C.
- In-field data site D.
- C, N and TOC results of the element analysis in the lab.

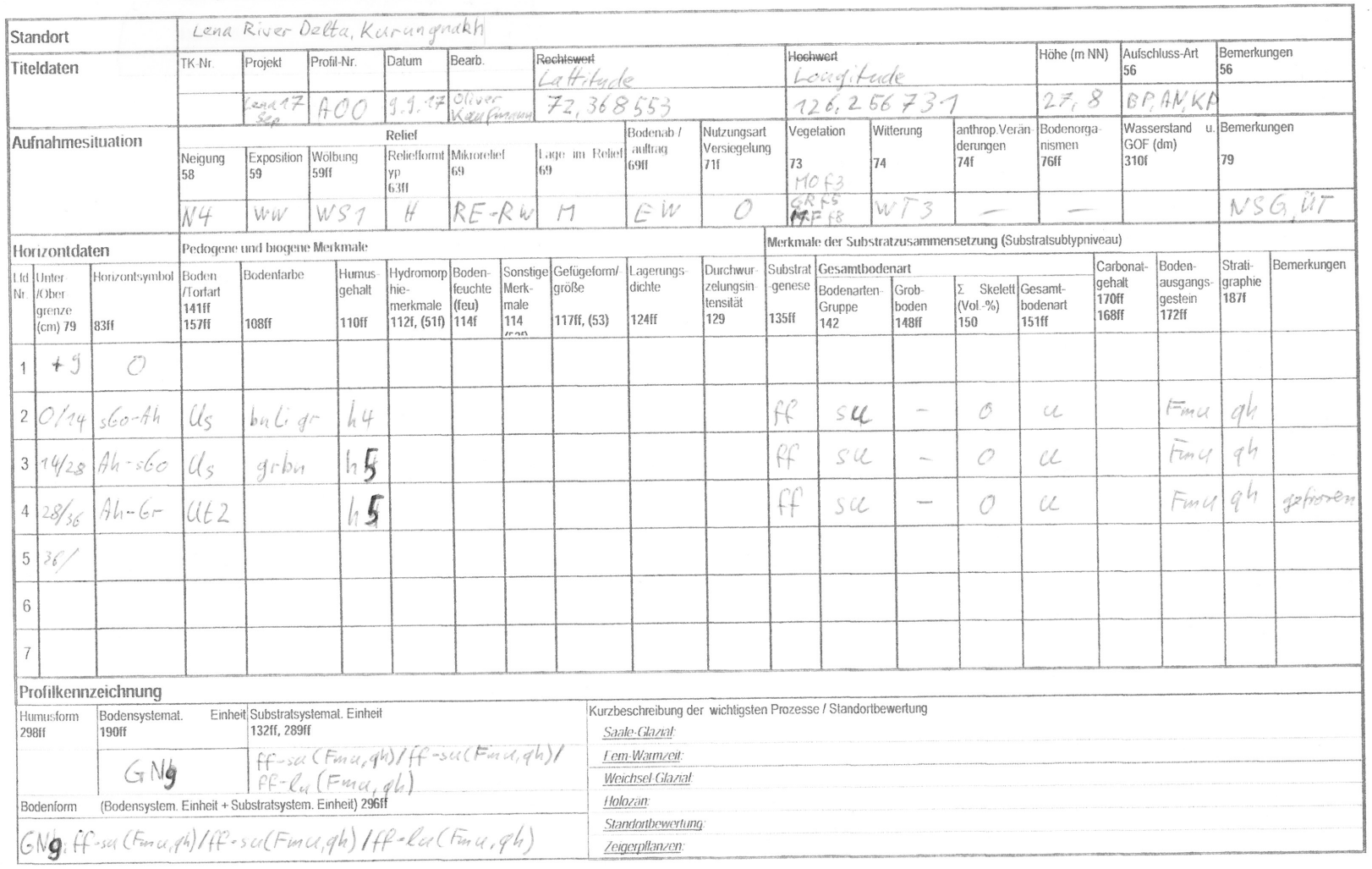

Standort	Lena River Delta, Kurungnakh																
Titeldaten	TK-Nr.	Projekt	Profil-Nr.	Datum	Bearb.	~~Rechtswert~~ Latitude				~~Hochwert~~ Longitude				Höhe (m NN)	Aufschluss-Art 56	Bemerkungen 56	
		Lena 17 Sep	A00	9.9.17	Oliver Kaufmann	72,368553				126,256731				27,8	BP, AM, KP		
Aufnahmesituation	Relief							Bodenab / auftrag 69ff	Nutzungsart Versiegelung 71f	Vegetation 73	Witterung 74	anthrop. Veränderungen 74f	Bodenorganismen 76ff	Wasserstand u. GOF (dm) 310f	Bemerkungen 79		
	Neigung 58	Exposition 59	Wölbung 59ff	Reliefformtyp 63ff	Mikrorelief 69	Lage im Relief 69				MOF3 GRF5 MF F8	WT3	—	—		NSG, ÜT		
	N4	WW	WS1	H	RE-RW	M		EW	O								

Horizontdaten			Pedogene und biogene Merkmale									Merkmale der Substratzusammensetzung (Substratsubtypniveau)								
Lfd Nr.	Unter-/Obergrenze (cm) 79	Horizontsymbol 83ff	Boden-/Torfart 141ff 157ff	Bodenfarbe 108ff	Humusgehalt 110ff	Hydromorphiemerkmale 112f, (51f)	Bodenfeuchte (feu) 114f	Sonstige Merkmale 114	Gefügeform/größe 117ff, (53)	Lagerungsdichte 124ff	Durchwurzelungsintensität 129	Substratgenese 135ff	Gesamtbodenart: Bodenarten-Gruppe 142	Grobboden 148ff	Σ Skelett (Vol.-%) 150	Gesamtbodenart 151ff	Carbonatgehalt 170ff 168ff	Bodenausgangsgestein 172ff	Stratigraphie 187f	Bemerkungen
1	+9	O																		
2	0/14	sGo-Ah	Us	bnLi gr	h4							ff	su	-	0	u		Fmu	qh	
3	14/28	Ah-sGo	Us	grbn	h5							ff	su	-	0	u		Fmu	qh	
4	28/36	Ah-Gr	Ut2		h5							ff	su	-	0	u		Fmu	qh	gefroren
5	36/																			
6																				
7																				

Profilkennzeichnung			
Humusform 298ff	Bodensystemat. Einheit 190ff	Substratsystemat. Einheit 132ff, 289ff	Kurzbeschreibung der wichtigsten Prozesse / Standortbewertung
	GNg	ff-su (Fmu, qh) / ff-su (Fmu, qh) / ff-lu (Fmu, qh)	*Saale-Glazial:*
Bodenform (Bodensystem. Einheit + Substratsystem. Einheit) 296ff			*Eem-Warmzeit:*
GNg: ff-su (Fmu, qh) / ff-su (Fmu, qh) / ff-lu (Fmu, qh)			*Weichsel-Glazial:*
			Holozän:
			Standortbewertung:
			Zeigerpflanzen:

Figure 11: In-field data site A

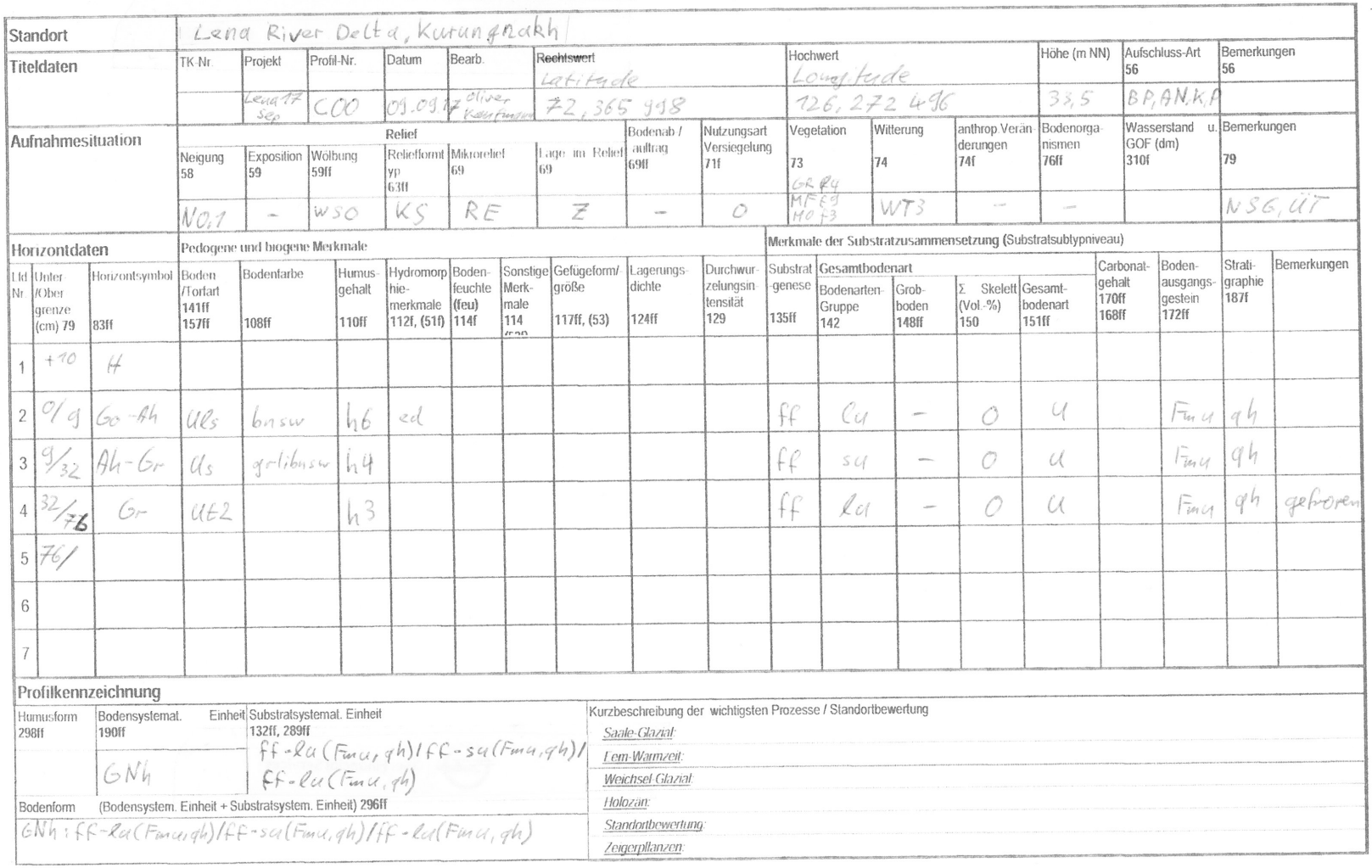

Standort	Lena River Delta, Kurungnakh																				
Titeldaten	TK-Nr.	Projekt	Profil-Nr.	Datum	Bearb.	Rechtswert					Hochwert					Höhe (m NN)	Aufschluss-Art 56	Bemerkungen 56			
		Lena 17 Sep	C00	09.09.17	oliver kruemmer	72, 365 998					126, 272 496					33,5	BP, AN, KP				
Aufnahmesituation	Relief								Bodenab / auftrag 69ff	Nutzungsart Versiegelung 71f	Vegetation 73	Witterung 74	anthrop. Veränderungen 74f	Bodenorganismen 76ff	Wasserstand u. GOF (dm) 310f	Bemerkungen 79					
	Neigung 58	Exposition 59	Wölbung 59ff	Reliefformtyp 63ff	Mikrorelief 69	Lage im Relief 69					GR R4 MF E3 HO F3	WT3	–	–		NSG, ÜT					
	NO,1	–	WSO	KS	RE	Z	–	O													
Horizontdaten	Pedogene und biogene Merkmale										Merkmale der Substratzusammensetzung (Substratsubtypniveau)										
Lfd Nr	Unter /Ober grenze (cm) 79	Horizontsymbol 83ff	Boden /Torfart 141ff 157ff	Bodenfarbe 108ff	Humusgehalt 110ff	Hydromorphiemerkmale 112f, (51f)	Bodenfeuchte (feu) 114f	Sonstige Merkmale 114	Gefügeform/größe 117ff, (53)	Lagerungsdichte 124ff	Durchwurzelungsintensität 129	Substratgenese 135ff	Gesamtbodenart: Bodenarten-Gruppe 142	Grobboden 148ff	Σ Skelett (Vol.-%) 150	Gesamtbodenart 151ff	Carbonatgehalt 170ff 168ff	Bodenausgangsgestein 172ff	Stratigraphie 187f	Bemerkungen	
1	+10	H																			
2	0/9	Go-Ah	Uls	brnsw	h6	ed						ff	Cu	–	0	u		Fmu	qh		
3	9/32	Ah-Gr	Us	grlibnsw	h4							ff	su	–	0	u		Fmu	qh		
4	32/76	Gr	Ut2		h3							ff	lu	–	0	u		Fmu	qh	gefroren	
5	76/																				
6																					
7																					

Profilkennzeichnung				
Humusform 298ff	Bodensystemat. Einheit 190ff	Substratsystemat. Einheit 132ff, 289ff	Kurzbeschreibung der wichtigsten Prozesse / Standortbewertung	
	GNh	ff-lu(Fmu, qh)/ff-su(Fmu, qh)/ ff-lu(Fmu, qh)	Saale-Glazial:	
Bodenform (Bodensystem. Einheit + Substratsystem. Einheit) 296ff			Eem-Warmzeit:	
GNh: ff-lu(Fmu, qh)/ff-su(Fmu, qh)/ff-lu(Fmu, qh)			Weichsel-Glazial:	
			Holozän:	
			Standortbewertung:	
			Zeigerpflanzen:	

Figure 12: In-field data site C

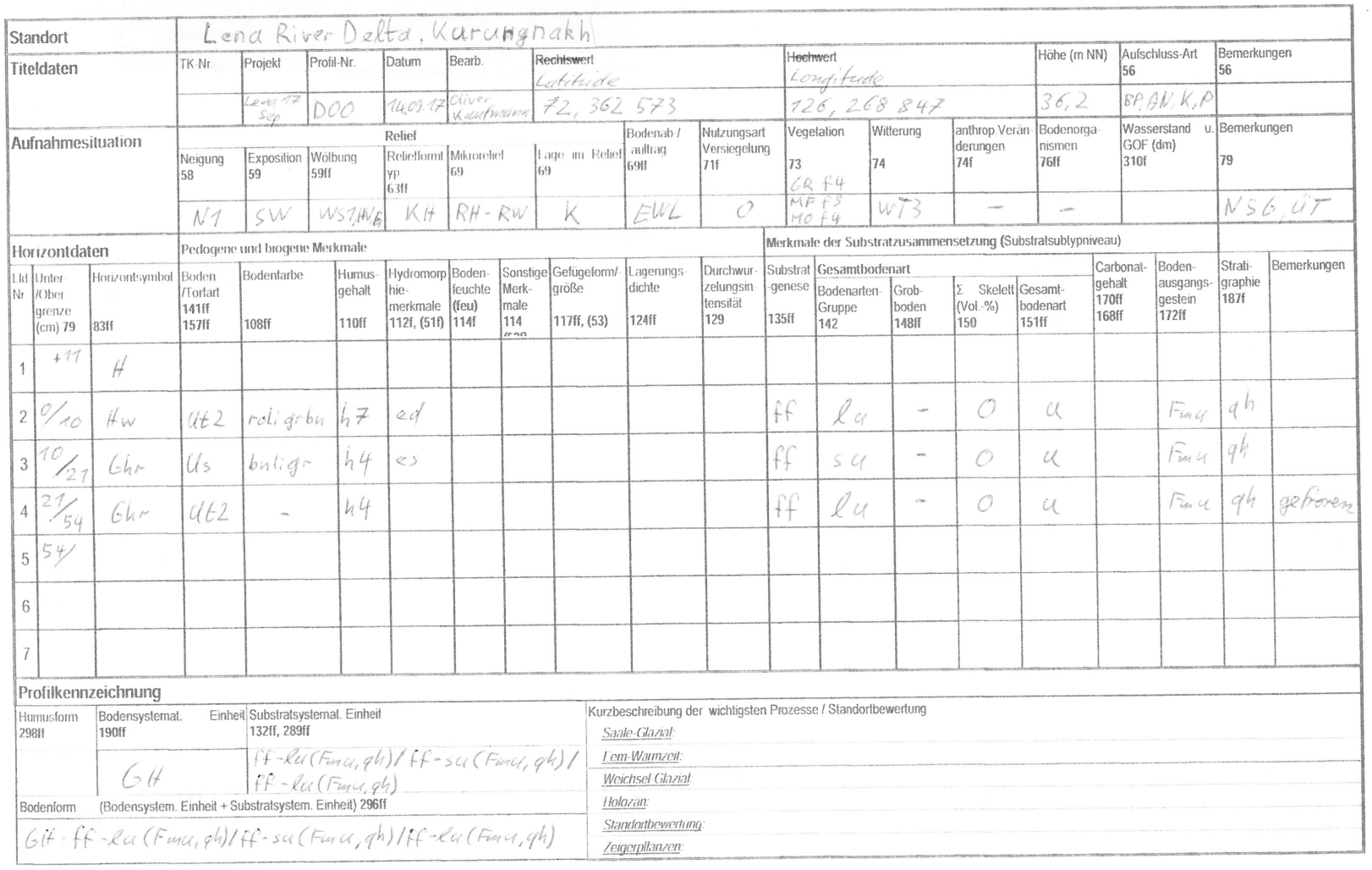

Standort	Lena River Delta, Kurungnakh																		
Titeldaten	TK-Nr.	Projekt	Profil-Nr.	Datum	Bearb.	Rechtswert Latitude				Hochwert Longitude				Höhe (m NN)	Aufschluss-Art 56	Bemerkungen 56			
		Lena 17 Sep	D00	14.09.17	Oliver Kaufmann	72, 362 573				126, 268 847				36,2	BP, AN, K, P				
Aufnahmesituation	Relief									Vegetation 73	Witterung 74	anthrop. Veränderungen 74f	Bodenorganismen 76ff	Wasserstand u. GOF (dm) 310f	Bemerkungen 79				
	Neigung 58	Exposition 59	Wölbung 59ff	Reliefformtyp 63ff	Mikrorelief 69	Lage im Relief 69	Bodenab / auftrag 69ff	Nutzungsart Versiegelung 71f		GR f4 MF f3 MO f4	WT3	–	–		NSG, UT				
	N1	SW	WS1, HW6	KH	RH-RW	K	EWL	O											

Horizontdaten			Pedogene und biogene Merkmale									Merkmale der Substratzusammensetzung (Substratsublypniveau)									
Lfd Nr	Unter-/Ober grenze (cm) 79	Horizontsymbol 83ff	Boden-/Torfart 141ff 157ff	Bodenfarbe 108ff	Humusgehalt 110ff	Hydromorphiemerkmale 112f, (51f)	Bodenfeuchte (feu) 114f	Sonstige Merkmale 114	Gefügeform/-größe 117ff, (53)	Lagerungsdichte 124ff	Durchwurzelungsintensität 129	Substratgenese 135ff	Gesamtbodenart Bodenarten-Gruppe 142	Grobboden 148ff	Σ Skelett (Vol.-%) 150	Gesamtbodenart 151ff	Carbonatgehalt 170ff 168ff	Bodenausgangsgestein 172ff	Stratigraphie 187f	Bemerkungen
1	+11	H																		
2	0/10	Hw	Ut2	rotlichgrau	h7	ed						ff	lu	-	0	u		Fmu	qh	
3	10/21	Ghr	Us	bunt	h4	es						ff	su	-	0	u		Fmu	qh	
4	21/54	Ghr	Ut2	-	h4							ff	lu	-	0	u		Fmu	qh	gefroren
5	54/																			
6																				
7																				

Profilkennzeichnung			
Humusform 298ff	Bodensystemat. Einheit 190ff	Substratsystemat. Einheit 132ff, 289ff	Kurzbeschreibung der wichtigsten Prozesse / Standortbewertung
	GH	ff-lu(Fmu, qh) / ff-su(Fmu, qh) / ff-lu(Fmu, qh)	*Saale-Glazial:*
Bodenform (Bodensystem. Einheit + Substratsystem. Einheit) 296ff			*Eem-Warmzeit:*
GH - ff-lu(Fmu, qh) / ff-su(Fmu, qh) / ff-lu(Fmu, qh)			*Weichsel-Glazial:*
			Holozän:
			Standortbewertung:
			Zeigerpflanzen:

Figure 13: In-field data site D

Proben/Exp./Name	Lena 2017 J. Nitzbon
Datum der Messung:	07.03.2018
Bearbeiter:	Oliver Kaufmann
Bemerkungen:	

Probenbezeichnung	N (%)	C (%)
A00 (71)	0,324	5,372
A00/2331	0,375	6,621
A00/2340	0,167	2,817
A00/2349	0,330	5,337
A00/2355	0,337	5,434
C00(75)	0,115	2,707
C01	0,156	3,497
C02	0,360	7,166
C03	0,353	7,654
C04	0,168	3,945
C05	0,271	5,984
C06	0,184	4,135
C07	0,217	4,838
C08	0,292	4,937
C09	0,162	3,606
C10	0,260	5,924
C00/218	0,155	3,526
C00/402	0,175	3,925
C00/837	0,707	11,006
C00/1337	0,889	16,601
D00(78)	0,173	3,526
D02(69)	0,238	4,613
D03(74)	0,292	4,939
D04(86)	0,215	4,134
D07(79)	0,727	13,353
D08(70)	0,539	9,147
D17(77)	0,147	4,002
D00(2333	1,182	19,127
D00/2337	0,141	3,654
D00/2347	1,367	22,720
D00/2359	0,139	3,601

Probenbezeic	TOC (%)
A00(71)	4,722
A00/2331	5,743
A00/2340	2,308
A00/2349	4,722
A00/2355	4,771
C00(75)	2,239
C01	3,028
C02	6,202
C03	6,630
C04	3,197
C05	5,003
C06	3,446
C07	4,040
C08	4,113
C09	2,907
C10	5,211
C00/218	2,795
C00/402	3,311
C00/837	9,281
C00/1337	14,415
D00(78)	2,821
D02(69)	3,741
D03(74)	4,141
D04(86)	3,538
D07(79)	11,202
D08 (70)	6,504
D17 (77)	3,154
D00/ 2333	17,031
D00/2337	2,984
D00/ 2347	20,139
D00/2359	2,807

Figure 14: C, N and TOC results of the element analysis in the lab.

Versicherung an Eides statt

Ich versichere an Eides statt, dass ich die vorliegende Arbeit im Studiengang Geowissenschaften selbstständig verfasst und keine anderen als die angegebenen Hilfsmittel – insbesondere keine im Quellenverzeichnis nicht benannten Internet-Quellen – benutzt habe. Alle Stellen, die wörtlich oder sinngemäß aus Veröffentlichungen entnommen wurden, sind als solche kenntlich gemacht.
Ich versichere weiterhin, dass ich die Arbeit vorher nicht in einem anderen Prüfungsverfahren eingereicht habe und die eingereichte schriftliche Fassung der auf dem elektronischen Speichermedium entspricht.

Ort, Datum	Unterschrift